Observation of phase boundaries in spontaneous optical pattern formation

Ming Shen,[1,2] Yonan Su,[1] Ray-Ching Hong,[1] YuanYao Lin,[1] Chien-Chung Jeng,[3] Ming-Feng Shih,[4] and Ray-Kuang Lee[1]

[1]*Institute of Photonics Technologies, National Tsing-Hua University, Hsinchu 300, Taiwan*

[2]*Department of Physics, Shanghai University, Shanghai 200444, China*

[3]*Department of Physics, National Chung-Hsing University, Taichung 402, Taiwan*

[4]*Department of Physics, National Taiwan University, Taipei 106, Taiwan*

(Received 6 November 2014; published 6 February 2015)

With measured optical images in spontaneous pattern formations, we observe the phase boundaries in the phase diagram, defining by the degree of coherence and biased voltage. Pattern transitions in the form of stripes, reoriented stripes, hexagons, and spots are revealed experimentally and theoretically for incoherent beams in noninstantaneous anisotropic photorefractive crystals, with demonstrations in the boundary of mixed-phase states.

DOI: 10.1103/PhysRevA.91.023810 PACS number(s): 42.65.Tg, 05.45.Yv, 42.70.Nq

I. INTRODUCTION

In optics, a small perturbation on top of plane waves growing exponentially during unidirectional propagation in nonlinear systems is known as modulation instability (MI) [1,2]. It is the MI that a broad optical beam or a quasi-cw (continuous wave) pulse breaks up into filaments or pulse trains, as a precursor to soliton formations [3,4]. Extending the uniformity into a quasi two-dimensional (2D) structure, another similar symmetry-breaking spontaneous pattern formation is associated with the transverse instability (TI) [5], which turns a bright soliton stripe into an array of 2D filaments [6–9], and bends a dark stripe into pairs of optical vortices [10]. Such a sequence of optical pattern transitions from MI to TI was recently demonstrated with a coherent beam propagating in the photorefractive crystals [11].

In addition to nonlinear optical systems, the appearance of these ordered patterns from an initially noisy and featureless background has been observed from spin class, catalysis, biology, geophysics, to cosmology, and been taken as a universal character in all scales [12]. Even though the accompanied growth of entropy with fluctuations should drive the physical system into disorder, it is believed that spontaneous pattern formations may happen associated with phase transitions. Recently, as Bose-Einstein condensate happens for atoms below a critical temperature, kinetic condensation in classical waves is observed in such a photorefractive crystal with the help of incoherent light [13]. In this work, with incoherent beams in noninstantaneous anisotropic photorefractive crystals [14–17], we report a series of pattern transitions in the form of stripes, reoriented stripes, hexagons, and spots experimentally and theoretically. By defining the phase diagram, in terms of coherence length and biased voltage, we demonstrate the observations of spontaneous optical patterns in the transition boundary of mixed-phase states. Through the detailed series of spontaneous pattern formations, the results in this work not only provide an important ingredient concerning the link with previous results on optical pattern formations, but also serve for the discussions on the underlying mechanisms for complex systems.

II. EXPERIMENTAL MEASUREMENT

Experimental setup for the measurement of our optical pattern transitions can be found in our previous work [11,16–18]. A 515 nm cw Yb:YAG laser output is split into two beams by using a polarization beam splitter, where the extraordinarily (signal) and ordinarily (background) polarized beams are collimated into a strontium-barium niobate (SBN) crystal as a control for the degree of saturation. Along the c axis, the SBN crystal is 5 mm in length and 5 mm in thickness, which has an effective electro-optical coefficient about 350 pm/V. The laser output passing through a diffusion glass, with the coherence length l_c estimated by the interference of speckle patterns, is launched on the input plane of the crystal. With a charge-coupled device (CCD) camera, a series of self-organized optical patterns at the output plane is recorded at a constant light intensity, i.e., $I_0 = 100\,\mathrm{mW/cm^2}$.

It was predicted theoretically first [19], then demonstrated experimentally [20,21], that with a noninstantaneous response in the nonlinear medium, such as the photorefractive crystal used in our experiments, MI can even occur with spatiotemporally incoherent white light when operating above a threshold. The threshold depends crucially upon the coherence property of input beam: The threshold increases when one decreases the spatial correlation distance. Below the threshold, perturbations on top of a uniform input beam decay and the related instability will be suppressed; while above the threshold, the perturbations grow rapidly and a uniform incoherent beam will break up into periodic stripes [22]. In experiments, first of all, we fix the biased voltage applying on the crystal at a constant value, $E_v = 0.93$ kV, and vary the coherence length of input beam to form spontaneous optical patterns with incoherent light. As the coherence length of the input beam increases, the measured patterns shown in Fig. 1 change from (a) uniform structure, into (b) stripes (coined as MI-1, primary MI), (c) a mixture of two kinds of stripes, and (d) reoriented stripes (coined as MI-2, secondary MI), (e) and (f) coexistence of stripes and hexagons, (g) hexagons (coined as TI), and (h) dots (coined as OT, optical turbulence), respectively.

Such a series of pattern transitions can be understood as follows. Beginning from a short coherence length, such as $l_c = 50\ \mu$m in Fig. 1(a), no spontaneous pattern appears due to the fact that the nonlinearity to support MI does not exceed the threshold value determined by the degree of coherence. Later on, as the degree of coherence is larger than the first threshold value to establish the primary MI (MI-1), as shown in Fig. 1(b)

 ©2015 American Physical Society

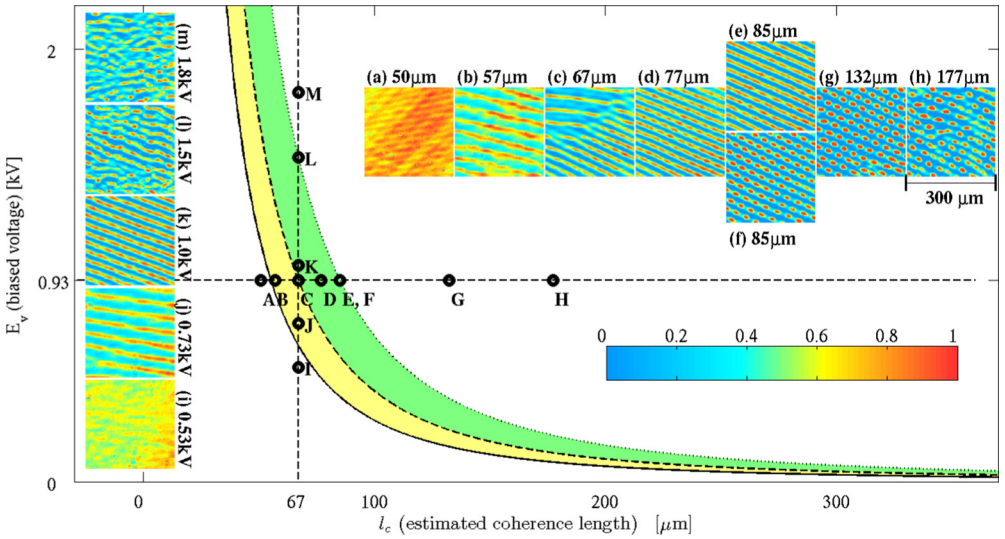

FIG. 1. (Color online) Parameter space in terms of coherence length l_c and biased voltage E_v for the spontaneous optical pattern formations, with primary MI (MI-1, yellow region), secondary MI (MI-2, green region), TI, and OT states. The insets show optical patterns captured by the CCD camera for (a)–(h) at a fixed biased voltage ($E_v = 0.93$ kV), but different coherence lengths, and (i)–(m) at a fixed coherence length ($l_c = 67$ μm), but different biased voltages. Each frame is 300 μm both in width and in height with the corresponding markers shown in capital letters. Theoretical curves in solid-, dashed-, and dotted lines depict the boundaries for MI-1, MI-2, and TI phases, respectively.

for $l_c = 57$ μm, stripe filaments in the periodic structure are developed with a random orientation. Increasing the coherence length above the second threshold value, one has the secondary MI pattern (MI-2) due to the anisotropy of crystals. By the comparison between optical patterns in Figs. 1(b) and 1(d), it can be clearly seen the difference between MI-1 and MI-2 states, i.e., the latter one has a reorientation of direction for the stripes (about 30°) along with a shrinking pitch between adjacent stripes. More interesting, we observe a mixed-phase state at $l_c = 67$ μm as shown in Fig. 1(c), just at the boundary of the MI-1 and MI-2 phase states, which demonstrates the coexistence of two phases. Consequently, these periodic stripes split and break up into 2D filaments as a result of incoherent TI at the third threshold of coherence length, $l_c = 85$ μm, at which another mixed-phase state of MI-2 and TI appears at random as shown in Figs. 1(e) and 1(f), respectively. When the input beam is more coherent, i.e., $l_c = 132$ μm, self-organized hexagon patterns as a manifestation of TI is demonstrated in Fig. 1(g). With a longer coherence length, the filament pattern forms in irregular spots representing a signature of OT, as shown in Fig. 1(h).

Instead of a fixed biased voltage, one can also operate the input light with a constant degree of coherence, for example, $l_c = 67$ μm in Fig. 1. Now, by increasing the biased voltage, again, we have a similar and detailed series of spontaneous pattern formations for incoherent light, as shown in Figs. 1(i)–1(m) with images from uniform background, stripes (MI-1), reoriented stripes (MI-2), hexagons (TI), to dots. Moreover, before the system involves into the optical turbulence state the region to observe MI or TI in an incoherent system becomes larger. In general, our experimental demonstrations verify such a universal behavior of spontaneous patten formations for incoherent MI and TI [23–25], but in a more subtle and complicated scenario.

III. THEORETICAL ANALYSIS FOR THE PHASE BOUNDARIES

To find out the threshold value as a function of coherence length and biased voltage for MI-1, MI-2, and TI states, we consider a 2D crystal with an anisotropy in nonlinearities. By adopting the incoherent matrix, one can find the most unstable spatial frequency, $k_j^{\max}$ $(j = x, y)$, for the perturbed field,

$$\frac{k_j^{\max}}{k_0} = \left[\frac{2n_j I_0}{n_0} - \frac{\theta_0^2}{2} - \left(\frac{2n_j I_0}{n_0}\theta_0^2 + \frac{\theta_0^4}{4}\right)^{1/2}\right]^{1/2}, \quad (1)$$

with the corresponding growth rate, g_j,

$$\frac{g_j}{k_0} = -\theta_0(k_j/k_0) + (k_j/k_0)\sqrt{\frac{n_j I_0}{n_0} - \left(\frac{k_j}{2k_0}\right)^2}, \quad (2)$$

where k_0 denotes the carrier wave number of incident beam, k_j $(j = x, y)$ denotes the perturbed wave number, $n_0 = 2.3$ is the refractive index, I_0 is the input intensity, n_j $(j = x, y)$ denotes the nonlinear index, and $\theta_0 \equiv \sqrt{2\pi}/k_0 n_0 l_c$ [19,23,26]. Here we also assume a Lorentzian power spectrum for the distribution of coherence, even though a Gaussian-type power spectrum determines the instability threshold physically in the experiment, but fails to give us an exact solution of the wave number and related growth rate. With the formulas in Eqs. (1) and (2), one can find two wave numbers with a maximum growth rate induced by the anisotropic nonlinearity for a given degree of incoherence, as shown in Figs. 2(a) and 2(b), respectively.

To model the anisotropy for the crystal, we estimate the ratio between the long and short axes of a nonlinear index ellipse as $n_x/n_y = 2.61$ for SBN crystals. Since $n_x > n_y$ is used, one can have the first threshold value for an incoherent beam to

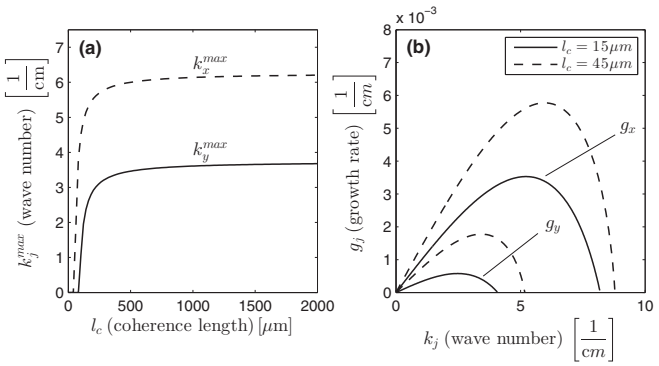

FIG. 2. (a) The most unstable wave number $k_j^{\max}$ as a function of the coherence length l_c along the x (dashed line) and y (solid line) directions in an anisotropic crystal. (b) The corresponding growth rate g_j is shown as a function of the wave number for different coherence lengths.

break up and form the pattern of stripes, i.e., the MI-1 phase, in one random direction (almost along the x axis). By increasing the coherence length, MI in another direction will reach its threshold condition subsequently and rotate the stripe pattern due to the superposition of wave vectors, $(k^{\max})^2 = (k_x^{\max})^2 + (k_y^{\max})^2$, resulting in shrinking the separation between adjacent stripes, $d = 1/k^{\max}$. Now, the system is in the MI-2 phase, which accounts for the observed optical patterns in shapes of reoriented stripes (superposition between two stripes). For the TI phase, we follow Ref. [7] by adding a small transverse wave number as the perturbation on top of the formed reoriented stripes, with the period derived from the MI gain spectrum. The resulting incoherent TI threshold condition can be found as $k_\rho/2n_0 = \theta_0^2$, where k_ρ denotes the wave number in the transverse direction. Based on the formula given above, we can theoretically define the threshold in terms of coherence length for TI.

In Fig. 1, we plot the corresponding threshold values of the MI-1, MI-2, and TI phases with respect to a given biased voltage (E_v) and coherence length (l_c) in solid, dashed, and dotted lines, respectively, by fitting the curves with the parameters mentioned above to experimental observations. The tendency of three threshold curves depicted in the parameter space defined by $E_v - l_c$, as shown in Fig. 1, demonstrates clearly that to have spontaneous pattern formations with an incoherent light source, one should increase the biased voltage to overcome the threshold condition. Moreover, as we have phase transitions in a low temperature system, the shadowed regions for supporting MI-1 and MI-2 phases are significantly narrowing as the degree of coherence increases, which explains why it is hard to observe the MI-2 phase with coherent light even in anisotropic crystals. In such a case, one would have a direct optical pattern transition from MI to TI states for a coherent light source, without revealing the phenomena of a secondary MI [11].

Before the conclusion, we want to remark that even though by considering the optical birefringence, it has been floating in the community for a long time that a 2D array of dot filaments should be viewed as the secondary MI due to the anisotropy of nonlinear crystals [22,26]. However, there are always some doubts that this relation truly exists. Through the demonstrations in experiment and theory, the above concerns are solved by our proposed phase diagram for pattern transitions in the form of MI-1 (primary MI in the form of stripes), MI-2 (secondary MI, reoriented stripes), TI (hexagons), and OT (optical turbulence in the form of spots). In particular, we introduce two different kinds of MI patterns, i.e., MI-1 and MI-2. Moreover, with the observations in the boundary of mixed-phase states as the critical temperature in a kinetic system, we provide clear evidence to explain the origin for the known 2D array of dot filament.

IV. CONCLUSION

In summary, we have demonstrated systematically the instabilities of MI-1 (primary MI in the form of stripes), MI-2 (secondary MI, reoriented stripes), TI (hexagons), and OT (optical turbulence in the form of spots) in noninstantaneous photorefractive crystals in detail with an incoherent light source. A phase diagram is proposed for optical phase transitions and observations of mixed-phase regimes in MI-1/MI-2 and MI-2/TI states are demonstrated at the phase boundaries. By adopting the incoherent matrix, theoretically we define the boundaries in the phase diagram, which gives good agreement with the experimentally measured optical images. By a detailed series of spontaneous optical pattern formations, our demonstrations open the pathway to a deeper insight into nonlinear optics and related phase transitions.

ACKNOWLEDGMENTS

This work is supported in part by the Ministry of Science and Technology, Taiwan, the Innovation Program of Shanghai Municipal Education Commission, and the Science and Technology Commission of Shanghai Municipal (Grant No. 15ZR1415700).

[1] V. I. Bespalov and V. I. Talanov, Filamentary structure of light beams in nonlinear liquids, JETP Lett. **3**, 307 (1966).
[2] V. I. Karpman, Self-modulation of nonlinear plane waves in dispersive media, JETP Lett. **6**, 277 (1967).
[3] M. I. Carvalho, S. R. Singh, and D. N. Christodoulides, Modulational instability of quasi-plane-wave optical beams biased in photorefractive crystals, Opt. Commun. **126**, 167 (1996).
[4] G. P. Agrawal, *Nonlinear Fiber Optics*, 2nd ed. (Academic Press, San Diego, 1995).
[5] Yu. S. Kivshar and D. E. Pelinovsky, Self-focusing and transverse instabilities of solitary waves, Phys. Rep. **331**, 117 (2000).
[6] A. V. Mamaev, M. Saffman, D. Z. Anderson, and A. A. Zozulya, Propagation of light beams in anisotropic nonlinear media: From symmetry breaking to spatial turbulence, Phys. Rev. A **54**, 870 (1996).

[7] C. Anastassiou, M. Soljacic, M. Segev, E. D. Eugenieva, D. N. Christodoulides, D. Kip, Z. H. Musslimani, and J. P. Torres, Eliminating the transverse instabilities of kerr solitons, Phys. Rev. Lett. **85**, 4888 (2000).

[8] Y. Y. Lin, R.-K. Lee, and Yu. S. Kivshar, Soliton transverse instabilities in nonlocal nonlinear media, J. Opt. Soc. Am. B **25**, 576 (2008).

[9] Y. Y. Lin, R.-K. Lee, and Yu. S. Kivshar, Transverse instability of transverse-magnetic solitons and nonlinear surface plasmons, Opt. Lett. **34**, 2982 (2009).

[10] A. V. Mamaev, M. Saffman, and A. A. Zozulya, Propagation of dark stripe beams in nonlinear media: Snake instability and creation of optical vortices, Phys. Rev. Lett. **76**, 2262 (1996).

[11] C.-C. Jeng, Y. Y. Lin, R.-C. Hong, and R.-K. Lee, Optical pattern transitions from modulation to transverse instabilities in photorefractive crystals, Phys. Rev. Lett. **102**, 153905 (2009).

[12] T. Shinbrot and F. J. Muzzio, Noise to order, Nature (London) **410**, 251 (2001).

[13] C. Sun, S. Jia, C. Barsi, S. Rica, A. Picozzi, and J. W. Fleischer, Observation of the kinetic condensation of classical waves, Nat. Phys. **8**, 470 (2012).

[14] M. Mitchell and M. Segev, Self-trapping of incoherent white light, Nature (London) **387**, 880 (1997).

[15] M. Mitchell, Z. Chen, M.-F. Shih, and M. Segev, Self-trapping of partially spatially incoherent light, Phys. Rev. Lett. **77**, 490 (1996).

[16] C.-C. Jeng, M.-F. Shih, K. Motzek, and Yu. Kivshar, Partially incoherent optical vortices in self-focusing nonlinear media, Phys. Rev. Lett. **92**, 043904 (2004).

[17] W.-H. Chu, C.-C. Jeng, C.-H. Chen, Y.-H. Liu, and M.-F. Shih, Induced spatiotemporal modulation instability in a noninstantaneous self-defocusing medium, Opt. Lett. **30**, 1846 (2005).

[18] M.-F. Shih, C.-C. Jeng, F.-W. Sheu, and C.-Y. Lin, Spatiotemporal optical modulation instability of coherent light in noninstantaneous nonlinear media, Phys. Rev. Lett. **88**, 133902 (2002).

[19] M. Soljacic, M. Segev, T. H. Coskun, D. N. Christodoulides, and A. Vishwanath, Modulation instability of incoherent beams in noninstantaneous nonlinear media, Phys. Rev. Lett. **84**, 467 (2000).

[20] D. Kip, M. Soljacic, M. Segev, E. Eugenieva, and D. N. Christodoulides, Modulation instability and pattern formation in spatially incoherent light beams, Science **290**, 495 (2000).

[21] T. H. Coskun, D. N. Christodoulides, Y.-R. Kim, Z. Chen, M. Soljacic, and M. Segev, Bright spatial solitons on a partially incoherent background, Phys. Rev. Lett. **84**, 2374 (2000).

[22] J. Klinger, H. Martin, and Z. Chen, Experiments on induced modulation instability of an incoherent optical beam, Opt. Lett. **26**, 271 (2001).

[23] D. Anderson, L. Helczynski-Wolf, M. Lisak, and V. Semenov, Features of modulational instability of partially coherent light: Importance of the incoherence spectrum, Phys. Rev. E **69**, 025601(R) (2004).

[24] D. Anderson, L. Helczynski-Wolf, M. Lisak, and V. Semenov, Transverse modulational instability of partially incoherent soliton stripes, Phys. Rev. E **70**, 026603 (2004).

[25] T. Schwartz, T. Carmon, H. Buljan, and M. Segev, Spontaneous pattern formation with incoherent white light, Phys. Rev. Lett. **93**, 223901 (2004).

[26] D. Kip, M. Soljacic, M. Segev, S. M. Sears, and D. N. Christodoulides, (1+1)-Dimensional modulation instability of spatially incoherent light, J. Opt. Soc. Am. B **19**, 502 (2002).